Astronomy & Astrophysics manuscript no. 1857˙draft˙mlg˙v2.1
November 1, 2011

Fermi-LAT constraints on the PWN nature of HESS J1857+026

R. Rousseau[1,2], M.-H. Grondin[3,4], A. Van Etten[5], M. Lemoine-Goumard[1,2], S. Bogdanov[6], J.W.T. Hessels[7,8], V. M. Kaspi[9], Z. Arzoumanian[6], F. Camilo[6], J. M. Casandjian[10], C. M. Espinoza[11], S. Johnston[12], A. G. Lyne[11], T. Reposeur[1], D. A. Smith[1], and B. W. Stappers[11]

(Affiliations can be found after the references)

Received /Accepted

ABSTRACT

Context. Since its launch, the Fermi satellite has firmly identified 5 pulsar wind nebulae plus a large number of candidates, all powered by young and energetic pulsars. HESS J1857+026 is a spatially extended γ-ray source detected by H.E.S.S. and classified as a possible pulsar wind nebula candidate powered by PSR J1856+0245.
Aims. We search for γ-ray pulsations from PSR J1856+0245 and explore the characteristics of its associated pulsar wind nebula.
Methods. Using a rotational ephemeris obtained from the Lovell telescope at Jodrell Bank Observatory at 1.520 GHz, we phase−fold 36 months of γ-ray data acquired by the Large Area Telescope (LAT) aboard Fermi. We also perform a complete γ−ray spectral and morphological analysis.
Results. No pulsation was detected from PSR J1856+0245. However, significant emission is detected at energies above 5 GeV at a position coincident with the TeV source HESS J1857+026. The γ-ray spectrum is well described by a simple power law with a spectral index of $\Gamma = 1.52 \pm 0.16_{\rm stat} \pm 0.55_{\rm syst}$ and an energy flux of $G(0.1-100\ {\rm GeV}) = (2.72 \pm 0.58_{\rm stat} \pm 1.51_{\rm syst}) \times 10^{-11}$ ergs/cm^2/s. This yields a γ−ray efficiency of $\sim$ 5 %, in the range expected for pulsar wind nebulae. Detailed multi-wavelength modeling brings new constraints on its pulsar wind nebula nature.

Key words. Pulsar Wind Nebula - Fermi-LAT - Gamma-Ray - HESS J1857+026 - PSR J1856+0245

1. Introduction

Pulsar wind nebulae (PWNe) are bubbles of shocked relativistic particles produced by the interaction of the pulsar's wind with the surrounding medium (Gaensler el al. 2006). Since 2003, the continuous observations of the Galactic Plane by Čerenkov telescopes have yielded the detection of more than 60 Galactic TeV sources. Among them, PWNe are the dominant class with 29 firm identifications. In the GeV energy range, 5 PWNe have been firmly identified by the Fermi-LAT. They are all powered by energetic pulsars and their γ-efficiencies are $\sim$ 1%, consistent with TeV observations (Ackermann et al. 2011; Grondin et al. 2011a).

The presence of a pulsar close to the source position is an important clue to confirm the identification of a PWN, which often requires information from the radio/X-ray wavelengths. Radio/X-ray PWNe are often associated with TeV extended sources offset from their pulsars, which can be explained by an inhomogeneous environment (Hinton et al. 2010). In such sources, TeV radiation can be explained by Inverse Compton (IC) scattering of accelerated leptons on ambient photon fields (CMB, IR, ...) or by π^0 decay from the interaction of accelerated hadrons with nuclei of the interstellar medium.

HESS J1857+026 is a very high energy (VHE) γ-ray source detected by HESS during the Galactic Plane Survey (Aharonian et al. 2008). The extended ($\sim 0.11°$) TeV source was identified as a PWN candidate after the discovery of PSR J1856+0245 (offset $\sim 0.12°$) in the Arecibo PALFA survey (Hessels et al. 2008). Recently, MAGIC reported a measured extension in the 0.2–1 TeV energy range significantly higher than the extension reported by H.E.S.S. at higher energies (Klepser et al. 2011). This might support the idea that low energy electrons from the PWN create the γ-ray signal after diffusing away from the pulsar. PSR J1856+0245 is an energetic pulsar ($\dot{E} = 4.6 \times 10^{36}$ erg/s) located in a crowded region, 1.3° from the bright SNR W44 (Abdo et al., 2010) and 0.6 ° from the fainter SNR HESS J1858+020 on which only an upper limit could be set using Fermi data (Torres et al. 2011). Significant emission coincident with HESS J1857+026 was observed above 100 GeV using Fermi-LAT observations (Neronov et al. 2010).

Here, we report in detail GeV observations of the HESS J1857+026/PSR J1856+0245 system using Fermi-LAT observations and discuss their implications for the nature of the source.

2. LAT description and data selection

The LAT is a gamma-ray telescope that detects photons by conversion into electron-positron pairs and operates in the energy range between 20 MeV and 300 GeV. Details of the instrument and data processing are given in Atwood et al., (2009). The on-orbit calibration is described in Abdo et al. (2009a).

The following analysis was performed using 36 months of data collected from August 4, 2008 to August, 31, 2011 within a 10×10 deg square around the position of HESS J1857+026. We excluded γ-rays coming from a zenith angle larger than 100° because of possible contamination from secondary γ-rays from the Earth's atmosphere (Abdo et al. 2009b). We used the P7 V6 Instrument Response Functions (IRFs), and selected the 'Source' events which correspond to a compromise between the number of selected photons and the background rate.

3. Data analysis

3.1. Timing analysis of PSR J1856+0245

With its large spin-down power, PSR J1856+0245 is one of the more energetic radio pulsars known. Its spin period of 80.9 ms and characteristic age of 20.6 kyr are similar to those of the

Vela pulsar. The dispersion measure and NE2001 electron density model of the Galaxy assign PSR J1856+0245 a distance of ∼ 9 kpc (Cordes et al. 2002).

This pulsar is not monitored as part of the LAT pulsar timing campaign (Smith et al. 2008), as it was discovered subsequently, but has nevertheless been regularly observed with the Lovell telescope at Jodrell Bank Observatory (Hobbs et al. 2004). The ephemeris of PSR J1856+0245 used in the analysis was obtained using 82 observations at 1.520 GHz made with the Lovell telescope between May 4, 2008 and September 04, 2011. The arrival times of events were corrected to the Solar System Barycenter using the JPL DE405 Solar System ephemeris. The TEMPO2 timing package (Hobbs et al. 2006) was then used to build the timing solution. We fit the radio times of arrival (TOAs) to the pulsar rotation frequency and first four derivatives (in order to remove timing noise). The post-fit rms is 1.081 ms, or 1.3 % of the pulsar phase. This timing solution will be made available through the Fermi Science Support Center[1] (FSSC).

For the LAT analysis, photons with energies above 100 MeV and within a radius of 1.0° of the radio pulsar position (α(J2000) = $18^h56^m50.937^s$, δ(J2000) = +02°45'47.046") were selected using an energy-dependent cone of radius $\theta_{68} < \max(5.12^\circ \times (E/100\,\mathrm{MeV})^{-0.8}, 0.2^\circ)$ and phase-folded using the radio ephemeris previously described. This choice takes into account the instrument performance and improves the signal to noise ratio over a broad energy range. The H-Test values obtained from the pulsed analysis correspond to a significance well below 2σ for each tested energy band (100 MeV – 300 GeV, 100 MeV – 300 MeV, 300 MeV – 1 GeV, > 1 GeV) (De Jager et al. 2009). Thus, no significant pulsation was detected.

3.2. Spatial and spectral analysis

Two different tools were used to perform the spatial and spectral analysis: `gtlike` and `pointlike`. `gtlike` is a binned maximum-likelihood method (Mattox et al. 1996) implemented in the Science Tools distributed by the FSSC. This tool fits a source model to the data along with models for the instrumental, extragalactic and Galactic components of the background. In the following analysis, the diffuse emission is modeled by the standard LAT diffuse emission models released by the Fermi Collaboration through the FSSC and described in Abdo et al. (2011). `pointlike` is an alternate binned likelihood technique that was extensively tested against `gtlike` (Kerr 2011). `pointlike` is optimized for characterizing the extension of a source (which is not the case for gtlike) and can be used to assess the Test Statistic (TS) value and derive the shape and spectra of both point-like and extended sources.

The TS measures the source significance and is defined as $TS = 2(L_1 - L_0)$, where L_1 corresponds to the log-likelihood obtained by fitting a model of the source of interest and the background model and L_0 correspond to the log-likelihood obtained by fitting the background model only.

Sources in a region of 15° around HESS J1857+026 from the Second Fermi-LAT catalog (Abdo et al. 2011) were taken into account in this study. Their spectral parameters were fixed if they were more than 5° from our source of interest. The region also includes the bright SNR W44 which could influence our fit. We refitted it assuming an elliptical ring and obtained results consistent with those of Abdo et al. (2010b).

[1] FSSC: http://fermi.gsfc.nasa.gov/ssc/data/access/lat/ephems/

3.2.1. Shape and position of HESS J1857+026 counterpart

Source shape analysis requires the best possible angular resolution. Since the source has a hard spectrum (see Section 3.2.2) we made a compromise between statistics and resolution by selecting photons above 10 GeV. This drastically reduces the contribution of the Galactic diffuse background. Fig. 1(a) presents a LAT TS Map in the energy range of 10 GeV to 300 GeV. The map contains the TS for a point source at each map location, thus giving a measure of the statistical significance for the detection of a γ-ray source in excess of the background. A source coincident with HESS J1857+026 is clearly visible.

We determined the spatial model of the source using `pointlike` with three different models : a point source, a uniform disk and a Gaussian. No significant extension was obtained above 10 GeV. The GeV emission was fit to position ($\alpha(J2000) = 18^h57^m14.4^s$, $\delta(J2000) = +02^\circ45'36.0$") with an average statistical error of 0.05°, consistent with the position determined by HESS ($\alpha(J2000) = 18^h56^m50.80^s$, $\delta(J2000) = +02^\circ45'50.2$").

3.2.2. Spectral analysis

Fig. 1(b) shows a TS map of the region in the energy range 0.1-1.3 GeV. There is an excess emission near HESS J1857+026 located at ($\alpha(J2000) = 18^h54^m19.2^s$, $\delta(J2000) = +02^\circ59'13.0$"). This excess is inconsistent with HESS J1857+026 and was added to the background model. This additional background source was fitted assuming a logarithmic parabola (eq. 2 in Abdo et al. (2011)), with spectral parameters $\alpha = 3.5 \pm 0.2_{stat}$, $\beta = 0.6 \pm 0.1_{stat}$, $E_0 \sim 1.2$ GeV, and $K = (3.1 \pm 0.5_{stat}) \times 10^{-12}$ ph/MeV/cm^2/s. Its significance above 300MeV is $\sim 4.6\sigma$.

Spectral analysis used with `gtlike`, selecting only 0.3-300 GeV to avoid the low energy range that is dominated by the diffuse Galactic background and subject to high systematics. In this energy range, HESS J1857+026 is well described by a pure power-law with an integrated flux extrapolated down to 100 MeV of F(0.1-100 GeV)=$(5.79 \pm 0.75_{\mathrm{stat}} \pm 3.11_{\mathrm{syst}}) \times 10^{-9}$ ph/cm^2/s, a spectral index of $\Gamma = 1.52 \pm 0.16_{\mathrm{stat}} \pm 0.55_{\mathrm{syst}}$ and an energy flux of G(0.1-100 GeV)=$(2.72 \pm 0.58_{\mathrm{stat}} \pm 1.51_{\mathrm{syst}}) \times 10^{-11}$ ergs/cm^2/s, which gives a significance of $\sim 6\sigma$ (TS=38.7).

Fermi-LAT spectral points for HESS J1857+026 were obtained by splitting the 0.3-300 GeV range into 4 logarithmically-spaced energy bins, as presented in Fig. 2. The errors on the spectral points represent the statistical and systematic errors added in quadrature. Three main systematic uncertainties can affect the LAT flux estimate for a point source: uncertainties in the Galactic diffuse background, uncertainties on the effective area and uncertainties on the true γ-ray morphology. We estimated these systematic errors as in Grondin et al. (2011b) and combined them in quadrature.

Assuming a distance of 9 kpc, the γ-ray flux corresponds to $L^{\gamma}_{PWN} = 2.49 \times 10^{35}$ ergs/s. Using the pulsar's $\dot{E}$, this yields a γ-ray efficiency of ∼ 5 %, which is one of the highest PWN efficiencies observed at GeV energies (Ackermann et al. 2011). It is still in the range of expected values, though, and confirms the trend observed in the TeV band (3.1 %) (Mattana et al. 2009; Marandon et al. 2010).

Using our best model of the region, we derived an upper limit on the DC emission of the pulsar. Following the procedure used by Romani et al. (2011), we added a point source at the position of the pulsar assuming a power-law of index 1.62 and a cut-off energy at 2.8 GeV. The 99% upper limit on the flux of 6.22 ×

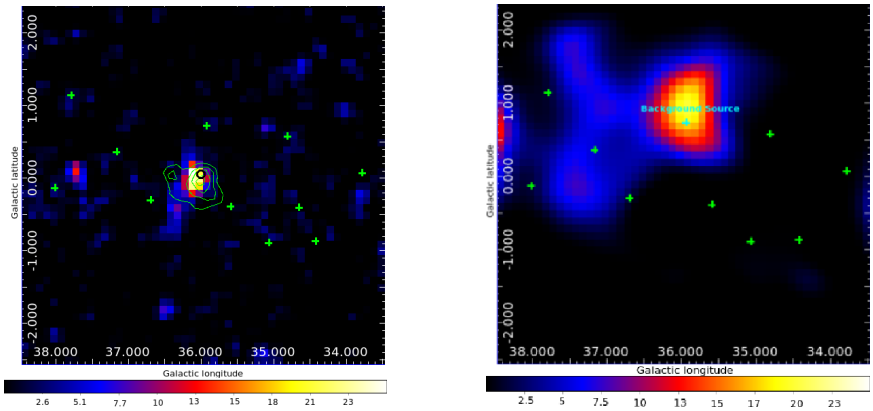

(a) (b)

Fig. 1. Residual TS maps obtained by fitting a source at each location of the map and computing the TS using `pointlike`. The green crosses represents the sources of the 2FGL catalog included in the model. Note that HESS J1857+026 is not included in the model. **(a):** Residual TS map obtained between 10 and 300 GeV. The green contours represent the HESS data (Aharonian et al., 2008). The position of the Fermi excess is consistent with that of HESS. The black circle represents the position of PSR J1856+0245. **(b):** Residual TS map obtained between 100 MeV and 1.3 GeV. This figure shows a residual excess taken into account in our model at the position of the cyan cross.

10^{-12} erg/cm^2/s implies a limit on the γ-ray luminosity of 7.47×10^{34} erg/s assuming a distance of 9 kpc.

4. Supporting X-Ray measurement

To obtain a precise flux for any potential X-ray PWN associated with PSR J1856+0245, we analyzed a 39-ks *Chandra* ACIS-I observation from 2011 February 28 (Obs. ID 12557). These data were recorded in the VFAINT and Timed Exposure (TE) modes and were analyzed using CIAO version 4.3.1 with CALDB 4.4.3. PSR J1856+0245 is clearly detected as a point source, but there was no immediate evidence for extended emission surrounding this position. Given that the size of the potential X-ray PWN is not known, we investigated two extraction regions to see whether they produce a statistically significant excess of counts compared with the background. These two extraction regions were in the form of annuli extending from $2'' - 7''$ and $2'' - 15''$ respectively from the position of the pulsar. The background regions were chosen from several other source free regions in the vicinity of the pulsar. For the $2'' - 7''$ extraction region we find an upper limit on the unabsorbed flux of 2×10^{-14} erg/s/cm^2 (1–10 keV, 3σ confidence), corresponding to a luminosity of 2×10^{32} erg/s. The background-subtracted counts in this region show a 1.7σ excess from zero. For the $2'' - 15''$ extraction region we find an upper limit on the unabsorbed flux of 5×10^{-14} erg/s/cm^2 (1–10 keV, 3σ confidence), corresponding to a luminosity of 5×10^{32} erg/s. The counts in this region show a 2σ excess from zero counts. Given the marginal significance of the count excesses in both cases we cannot convincingly claim the detection of a weak X-ray PWN. These luminosity limits are derived from the 3σ upper bound on the net count rate and assume a typical powerlaw spectrum of index 1.5 for the PWN, a distance of 9 kpc, and a column density $N_{\rm H} = 4\times10^{22}$ cm^{-2}. An in-depth analysis of the X-ray properties of PSR J1856+0245 will be presented elsewhere.

5. Discussion

To investigate the global properties of the PWN, we apply a one-zone time dependent SED model which reproduces the multi-wavelength measurements from MAGIC (Klepser et al. 2011), H.E.S.S. (Aharonian et al. 2008), as well as the LAT and the $2'' - 15''$ X-ray upper limit described above. This model, described in Grondin et al. (2011b) and Abdo et al. (2010a), computes SEDs from evolving electron populations over the lifetime of the pulsar in a series of time steps. During the free-expansion phase of the PWN (assumed to be $\sim 10^4$ years) we adopt an expansion of $R \propto t$, following which the radius evolves as $R \propto t^{0.3}$, appropriate for a PWN expanding in pressure equilibrium with a Sedov phase SNR. Over the pulsar lifetime the magnetic field evolves as $B \propto t^{-1.5}$, following ~ 500 years of constancy. We fix the pulsar braking index to the canonical value of 3.

We assume the existence of three primary photon fields (CMBR, far IR (dust), and starlight) and use the interstellar radiation mapcube within the GALPROP suite (Porter et al. 2005) to estimate the photon fields at the Galactic radius of PSR J1856+0245. A distance of 9 kpc in the direction of the pulsar corresponds to a Galactic radius of 5.4 kpc. At this radius, the peak of the SED of dust IR photons corresponds to a black body temperature of $T \sim 32$ K with a density of ~ 1.1 eV cm^{-3}, while the SED of stellar photons peaks at $T \sim 2500$ K with a density of ~ 1.2 eV cm^{-3}.

A simple exponentially cutoff power-law injection of electrons, evolved properly over the pulsar lifetime, often provides an adequate match to PWNe SEDS. For this injection spectrum we fit four variables: final magnetic field $B_{\rm f} = 0.8 \pm 0.4\,\mu$G, electron high energy cutoff $E_{\rm cut} = 66 \pm 16$ TeV, electron power-law index $p = 2.25 \pm 0.03$, and initial pulsar spin period $P_0 = 9.9 \pm 6.1$ ms, which gives an age of 20 kyr. This model yields a $\chi^2/dof = 23.9/21$ and poorly matches the low energy MAGIC points, as shown in Figure 2 (Left).

Another option to fit the multi-wavelength data is to adopt the relativistic Maxwellian plus power-law tail electron spectrum proposed by Spitkovsky (2008). We implement this spectrum as described in Grondin et al. (2011b). The best fit, presented in Fig. 2 (Middle), is obtained with $kT = 0.96 \pm 0.17$ TeV corresponding to an upstream gamma-factor of 3.7×10^6, a magnetic field of $B_{\rm f} = 1.0 \pm 0.9\,\mu$G, a cutoff at $E_{\rm cut} = 92 \pm 26$ TeV and a power-law index of $p = 2.45 \pm 0.12$, consistent with the value of ~ 2.5 proposed by Spitkovsky (2008). The braking index of $n = 3$ and initial spin period of $P_0 = 48 \pm 4$ ms give an age of 13 kyr. The relativistic Maxwellian plus power law model better matches the multi-wavelength data, with a $\chi^2/dof = 13.6/20$. A hadronic scenario is also possible, with γ-rays arising from

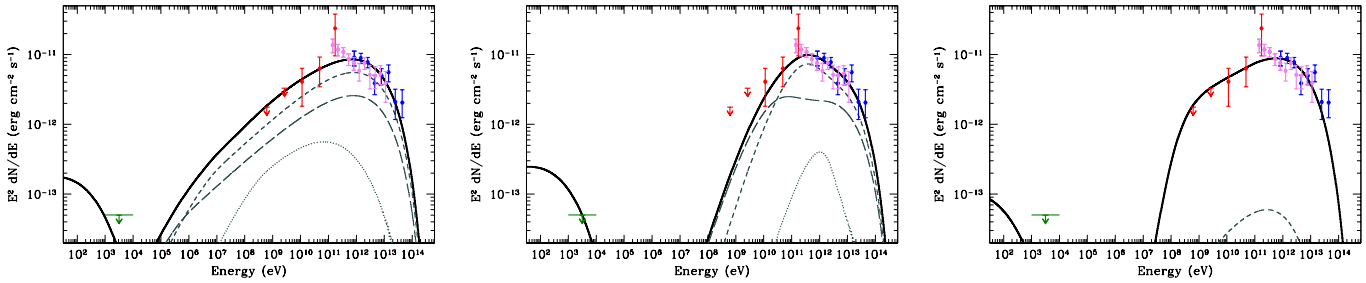

Fig. 2. Spectral energy distribution of HESS J1857+026 with a simple exponentially cutoff power-law electron spectrum (a), a relativistic Maxwellian plus power-law electron spectrum (b), and an exponentially cutoff power-law proton spectrum (c). The X-ray flux point (green), LAT spectral points (red), MAGIC points (violet) (Klepser et al. 2011), and H.E.S.S. points (blue) (Aharonian et al. 2008) are shown. The black line denotes the total synchrotron, inverse Compton and pion decay emission from the nebula.Thin curves indicate the Compton components from scattering on the CMB (long-dashed), IR (medium-dashed), and stellar (dotted) photons.

proton-proton interactions and subsequent pion decay. For this model, corresponding to Fig. 2 (Right), we fix the ambient gas density at $50\,\mathrm{cm}^{-3}$ and age at 20 kyr. We find a best fit of $\chi^2/dof = 24.7/21$ with a magnetic field of $B_\mathrm{f} = 10 \pm 20\,\mu$G, proton cutoff at $E_\mathrm{p,cut} = 73 \pm 27$ TeV, a proton power-law index of $p = 1.83 \pm 0.03$, and an energy content in protons of $6.9 \pm 0.6 \times 10^{49}$ erg.

The MAGIC and H.E.S.S. data combine to form a power-law spectra of index ~ 2.3 over nearly three decades in energy. This VHE data, combined with the limits imposed by the steep LAT data, is difficult to match with a simple power-law injection of electrons (or protons), and we find a significantly better fit with a relativistic Maxwellian plus power-law spectrum. Yet the exceedingly low magnetic field of the leptonic fits, due to the stringent X-ray upper limit, call into question these models. Such a low magnetic field implies that if PWN leptons are indeed responsible for the γ-ray flux, they must be dominated by relic electrons which have escaped the PWN core into very weakly magnetized surroundings. The hadronic scenario relaxes this constraint, though the energy requirements are quite high even for a dense ambient medium, and a very hard power-law index is required. At present the true nature of HESS J1857+026 remains a mystery, though the new LAT data and X-ray upper limit hint that this source is far from a typical TeV PWN.

Acknowledgements

The *Fermi* LAT Collaboration acknowledges support from a number of agencies and institutes for both development and the operation of the LAT as well as scientific data analysis. These include NASA and DOE in the United States, CEA/Irfu and IN2P3/CNRS in France, ASI and INFN in Italy, MEXT, KEK, and JAXA in Japan, and the K. A. Wallenberg Foundation, the Swedish Research Council and the National Space Board in Sweden. Additional support from INAF in Italy and CNES in France for science analysis during the operations phase is also gratefully acknowledged.

The Lovell Telescope is owned and operated by the University of Manchester as part of the Jodrell Bank Centre for Astrophysics with support from the Science and Technology Facilities Council of the United Kingdom.

References

A. Abdo et al., ApJ, 696, 2, 1084-1093, 2009 a
A. Abdo et al., Phys. Rev. D, 80, 122004, 2009 b
A. Abdo et al., ApJ, 713, 146, 2010 a
A. Abdo et al., Science, 327, 1103-1106, 2010 b
A. Abdo et al., ApJS, Submitted, 2011
M. Ackermann et al., ApJ, 726, 35, 2011
F. Aharonian et al., A&A, 477, 353, 2008
W. Atwood et al., ApJ, 697, 2, 1071-1102, 2009
J. Cordes, T. Lazio, arXiv:astro-ph/0207156
J. Fang, & Zhang, L. A&A, 515, A20, 2010
0. De Jager et al., A&A, 221, 180, 1989
B. Gaensler, P. Slane, Ann. Rev. of A & A, 44, 17-47, 2006.
M.-H. Grondin, M. Lemoine-Goumard, Heep conf., A.S.S.P., 399-411, 2011 a
M.-H. Grondin et al., ApJ, 738, 42, 2011 b
J.A. Hinton and W. Hofmann, Ann. Rev. A& A, 47, 523-565, 2010
G. Hobbs et al., MNRAS 353, 1311, 2004
G. Hobbs et al., Chin. J. A A, 6, 2, 189, 2006
J. Hessels et al., ApJ, 682, L41–L44, 2008
M. Kerr, arXiv:1101.6072v
S. Klepser et al., proc. 32 ICRC : arXiv:1109.6448v1
V. Marandon et al., thesis, 2010
F. Mattana et al., ApJ, 694, 12-17, 2009
J. Mattox et al., ApJ, 461, 396-407, 1996
A. Neronov et al., arXiv:1011.0210v1
T. A. Porter et al., International Cosmic Ray Conference, 4, 77, 2005
R. Romani et al., arXiv:1106.5762v1
P. Slane et al., ApJ, 720, 266, 2010
D. A. Smith et al., A&A, 492, 3, 923-931, 2008
A. Spitkovsky, ApJ, 682, L5, 2008
D. Torres et al., arXiv:1107.3470

[1] Centre d'Études Nucléaires de Bordeaux Gradignan, IN2P3/CNRS, Université Bordeaux 1, BP120, F-33175 Gradignan Cedex, France
[2] Funded by contract ERC-StG-259391 from the European Community
[3] Max-Planck-Institut für Kernphysik, D-69029 Heidelberg, Germany
[4] Landessternwarte, Universität Heidelberg, Königstuhl, D 69117 Heidelberg, Germany
[5] W. W. Hansen Experimental Physics Laboratory, Kavli Institute for Particle Astrophysics and Cosmology, Department of Physics and SLAC National Accelerator Laboratory, Stanford University, Stanford, CA 94305, USA
[6] Columbia Astrophysics Laboratory, Columbia University, New York, NY 10027, USA
[7] The Netherlands Institute for Radio Astronomy (ASTRON),Postbus 2, 7990 AA Dwingeloo, Netherlands
[8] Astronomical Institute "Anton Pannekoek" University of Amsterdam, Postbus 94249 1090 GE Amsterdam, Netherlands
[9] Department of Physics, McGill University, Montreal, PQ, Canada H3A 2T8
[10] Laboratoire AIM, CEA-IRFU/CNRS/Université Paris Diderot, Service d'Astrophysique, CEA Saclay, 91191 Gif sur Yvette, France
[11] Jodrell Bank Centre for Astrophysics, School of Physics and Astronomy, The University of Manchester, M13 9PL, UK

[12] CSIRO Astronomy and Space Science, Australia Telescope National Facility, Epping NSW 1710, Australia
e-mail: rousseau@cenbg.in2p3.fr, Marie-Helene.Grondin@mpi-hd.mpg.de, ave@stanford.edu, lemoine@cenbg.in2p3.fr